

# Open Research Online

---

The Open University's repository of research publications and other research outputs

## Assessing atmospheric predictability on Mars using numerical weather prediction and data assimilation

### Conference or Workshop Item

How to cite:

Rogberg, P.; Read, P. L. and Lewis, S. R. (2008). Assessing atmospheric predictability on Mars using numerical weather prediction and data assimilation. In: Third International Workshop on The Mars Atmosphere: Modeling and Observations, 10-13 Nov 2008, Williamsburg, Virginia, pp. 1-4.

For guidance on citations see [FAQs](#).

© [not recorded]

Version: [not recorded]

Link(s) to article on publisher's website:  
<http://www.lpi.usra.edu/meetings/modeling2008/>

---

Copyright and Moral Rights for the articles on this site are retained by the individual authors and/or other copyright owners. For more information on Open Research Online's data [policy](#) on reuse of materials please consult the policies page.

---

[oro.open.ac.uk](http://oro.open.ac.uk)

**ASSESSING ATMOSPHERIC PREDICTABILITY ON MARS USING NUMERICAL WEATHER PREDICTION AND DATA ASSIMILATION** P. Rogberg<sup>1</sup>, P. L. Read<sup>1</sup>, S. R. Lewis<sup>2</sup>, L. Montabone<sup>2,3</sup>

<sup>1</sup>University of Oxford, Dept. of Physics, Atmospheric, Oceanic and Planetary Physics, Oxford, UK ([p.read1@physics.ox.ac.uk](mailto:p.read1@physics.ox.ac.uk)), <sup>2</sup>The Open University, Dept. of Physics and Astronomy, Milton Keynes, UK, <sup>3</sup>Université Paris VI, Laboratoire de Météorologie Dynamique, Paris, France

**Introduction:** Studies of the time series of surface measurements of wind, pressure and temperature at the two Viking landers by Barnes [1], [2] revealed that baroclinic transient travelling waves on Mars occur mostly during northern hemisphere autumn, winter and early spring, and typically take the form of highly coherent patterns with planetary wavenumbers 1-3 that can persist for intervals of up to 30-60 sols before changing erratically. Such behaviour is almost unknown on Earth, where individual baroclinic weather systems typically persist for no longer than 5-10 days and seldom remain coherent around entire latitude circles. This occurrence of planetary-scale coherent baroclinic wave-like weather systems on Mars led to suggestions [3] that Mars' atmospheric circulation operates in a quite different dynamical regime to that of the Earth, one that tends to favour regular, symmetrical baroclinic wave activity in a manner reminiscent of the regular wave regimes found in laboratory fluid dynamics experiments on sloping convection in a rotating, thermally-driven fluid annulus (e.g. [4], [5]). In its extreme form, this hypothetical comparison would suggest the possibility of a fully non-chaotic atmospheric circulation on Mars, though subsequent modelling work [6] indicated that perturbations due to the thermal tide would lead to chaotic transitions back and forth between different intransitive wave states. This form of (relatively low-dimensional) chaotic mode-flipping appeared to be consistent with the Viking observations of Mars, suggesting nevertheless that the intrinsic predictability of Mars' mid-latitude meteorology was qualitatively and quantitatively quite different from that of the Earth.

Most recently, Newman et al. [7] have attempted to quantify the intrinsic predictability of the large-scale atmospheric circulation on Mars (at least in the absence of significant dust storms), and its seasonal variability, by applying methods of ensemble weather prediction and 'breeding vectors' [8] to numerical simulations of Martian meteorology. Such methods directly address the sensitivity of chaotic atmospheric behaviour to initial conditions by running a set of simulations in parallel from a closely similar (though non-identical) set of initial conditions, typically derived by perturbing a fully three-dimensional atmospheric state obtained from a previous simulation. Newman et al.

[7] found that forecast ensembles would only diverge typically during northern hemisphere autumn and winter, with e-folding timescales of 3-8 sols. The patterns of divergence were consistent with chaotic behaviour dominated by the action of planetary scale baroclinic waves at middle and high northern latitudes, much as found to dominate the actual circulation during these seasons. At other seasons, perturbations to the forecasts were often found not to grow, provided the perturbation was sufficiently large, suggesting that, at least on large scales, the Martian atmosphere was non-chaotic (even in the presence of diurnal tides, topography and other complex features). During the latter seasons, however, baroclinic activity in the northern hemisphere was virtually absent, although some weaker baroclinic transients were found during the southern hemisphere autumn and winter seasons. These did not, however, appear to lead to sustained chaotic divergence of model forecasts.

A major limitation of the previous study by Newman et al. [7] was that it took no account of sources of variability other than internal nonlinear interactions and external periodic forcing. In particular, the dust distribution in the model simulations was prescribed externally, so that, in the absence of baroclinic wave activity, the simulated meteorology was relatively quiescent in response to the highly predictable (seasonal and diurnal) external forcing. In the present study, therefore, we have extended this ensemble prediction approach to investigate the intrinsic *and practical* predictability of a more realistic system, as represented in assimilated analyses of observations of Mars itself [9 – 11]. This allows us to obtain more complete and realistic atmospheric states from which to initialise deterministic forecasts, for which variability of dust and other aspects not included in the baseline version of the GCM is taken into account. In this paper, therefore, we examine the typical growth rates of perturbations in ensemble predictions of Martian meteorology, initialised from observed states and predicted using more realistic distributions of atmospheric dust, again derived from observations. Error growth is considered both with respect to the intra-ensemble spread as the forecast progresses, and with respect to observations subsequent to the initial state (an observational verification of the forecast). The latter turns out to be a par-

ticularly stringent test of model performance, and serves to expose a number of systematic errors in the standalone model climatology.

**Intra-ensemble error growth:** A series of numerical forecast experiments were initialized from particular timesteps in a re-analysis dataset of the Martian atmosphere, obtained by assimilating Mars Global Surveyor/Thermal Emission Spectrometer (TES) retrieved profiles of temperature and total dust optical depth into the UK Mars General Circulation Model (MGCM) [9-11]. A single timestep was chosen to sample each of the 12 main ‘seasons’ of each of MY 25 and 26, representing a ‘normal’ Martian year (MY26) and one with a planet-encircling dust storm (MY25). The model used for the forecast was the UK version of the European MGCM[12], using parameters appropriate to the ‘typical’ MGS year. The horizontal dust distribution, however, was taken from the observed state obtained from TES measurements, using the TES map of total dust optical depth extended into the vertical using simple analytical functions with the top of the dust layer specified as a function of latitude and time of year (cf [10,12]). To generate an ensemble of initial perturbed states we used the approach of Houtekamer & Derome[13] in constructing pairwise sets of two-member ensembles, i.e. initial states were produced in pairs by respectively adding and subtracting a given perturbation pattern to the basic analysed field. Houtekamer & Derome [13] showed that using symmetrically distributed initial states is an efficient way of creating initial states for ensemble members in that they tend to enclose the ‘true’ solution and thus minimise the ensemble size. The baseline initial state was perturbed by adding random noise of rms amplitude 5 K to the temperature field. Ensembles initialized in this manner were then integrated forward for up to 30 sols. The ensemble spread was measured by determining the rms temperature difference  $\Delta T$  on the 30 Pa pressure surface between the unperturbed forecast and perturbed ensemble members.

Fig. 1 shows an example of the growth of perturbations from the initial state. The perturbations initially decay during the first sol or so, as the model adjusts to the added noise, and then grow fairly rapidly over the ensuing 3-5 sols before equilibrating to an amplitude of ~2-3 K after ~ 10 sol. This growth is typical of NH winter, in which chaotic growth is dominated by the behaviour of strong baroclinic transients surrounding the north pole.

The growth of perturbations is roughly exponential during the early (post-transient) stages of each forecast, of the form

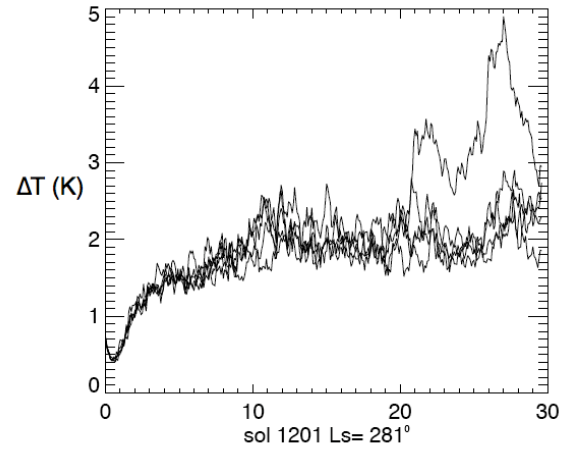


Figure 1: Growth of ensemble spread in terms of rms temperature differences between ensemble members on the 30 Pa pressure surface, averaged over the globe. Example shown for  $L_s = 281^\circ$  in MY25.

$$\Delta T \sim T_0 \exp[\gamma t], \quad (1)$$

so the mean growth rate  $\gamma$  can be determined by fitting a simple exponential growth curve to  $\Delta T(t)$  between sols 1-4 of each forecast. The results are shown in Fig. 2 for each season of both MY25 and MY26. Results are fairly consistent for both MY25 and MY26, though unlike the cases found by Newman et al.[7], perturbations are found to grow significantly even during northern summer. This may reflect the presence of more active baroclinic weather systems in the SH during southern winter in the assimilated observations than reproduced in the standalone model.

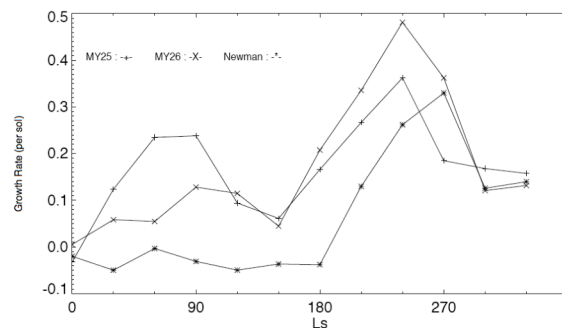


Figure 2: Mean growth rate of disturbances (in  $\text{sol}^{-1}$ ) as a function of time of year, showing results for ensembles initialized during MY 25, MY 26 and in the standalone model study by Newman et al.[7].

**Forecast verification against reanalyses:** A more stringent test of the predictive skill of the UK MGCM

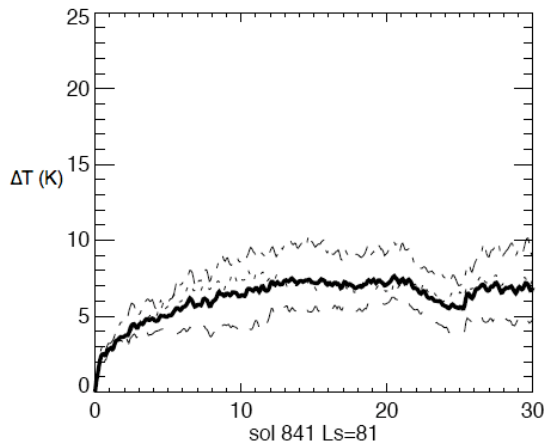


Figure 3: RMS temperature difference on the 30 Pa surface between model forecast and subsequent assimilated analysis for the 30 sols following the initial state. Solid line shows  $\Delta T$  averaged over the entire globe, while dashed, dash-dotted and dotted lines indicate  $\Delta T$  averaged over the NH, EQ and SH latitude bands.

is provided by direct comparison between the (unperturbed) model forecast and the subsequent assimilated analyses during the 30 sols following the forecast initialisation.

Fig. 3 shows the growth of model ‘forecast error’ from an initial state during MY25 close to NH summer solstice. This shows fairly typical behaviour found at most seasons, in which the model forecast rapidly departs from the observed state during the first 1-2 sols. The model error now grows to much larger amplitude than found within the model-only ensembles, reaching amplitudes of 5-10 K, but with significant regional variability. In this case, the dominant region contributing to divergence of the forecast from observations is the low-latitude EQ band, with somewhat weaker growth at mid-high latitudes in both hemispheres (though is least in the northern summer midlatitudes).

This would seem to reflect a clear tendency for the model to drift away from the observed state with a growth rate of around  $2 \text{ sol}^{-1}$ . This growth rate is found more or less at all times of year, and is consistent with the adjustment of the model state towards a new radiative-dynamical equilibrium on the radiative relaxation timescale typical of the Martian lower atmosphere [14] of around 0.3-0.5 sol. This is, in effect, a form of radiative ‘climate drift’ that, on Mars, takes place well within the time frame normally associated on Earth with weather forecasting. This would seem to indicate that accurate, deterministic practical forecasts of Mar-

tian weather actually require extremely accurate representations of radiative forcing processes within the atmosphere. Such representations in practice would need an accurate knowledge not only of the radiative parameters for infrared radiative transfer by  $\text{CO}_2$ , but also of the 3D time-varying distribution of dust and other radiatively active aerosols within the atmosphere.

In the present case, the radiative transfer scheme used in the UK MGCM has some known systematic errors in its heating and cooling rates, in common with other versions of the European MGCM, and only limited information was available on the spatial distribution of suspended dust. In fact the dust distribution was held fixed and identical to the distribution in the initial state during each forecast, and so gradual drift away from the observed state is bound to take place at some point during the forecast as the assumed dust distribution becomes less and less realistic.

At this particular time of year, around  $L_S \sim 80^\circ$ - $120^\circ$ , a band of water ice clouds is observed to develop at low latitudes, in association with a cooling of the global atmosphere close to aphelion. A recent study [15] has shown that the climatological state predicted by MGCMs that do not include a representation of the radiative effects of water ice clouds will lead to significant errors  $\sim 5$ - $10\text{K}$  in simulated atmospheric temperature, especially around 10-100 Pa and at low latitudes. Such errors were clearly identified in comparisons with assimilated analyses.

*An empirically-corrected forecast.* A potential implication of the above result is that it should be possible to greatly improve the accuracy of deterministic forecasts if systematic errors in the model parameterization schemes can be corrected. In order to test the sensitivity of this approach, we have made a test forecast using the UK MGCM in which a simple relaxation correction term of the form  $(T_A - T_M)/\tau$  was added to the prognostic equation for temperature in the model, where  $T_A$  is the zonal mean temperature field in the assimilated analysis, averaged over the 30 sol period of the forecast,  $T_M$  is the zonal mean model-predicted temperature without correction, and  $\tau$  is a tunable constant controlling the strength of the correction being applied. This effectively forms an empirical correction applied only to the zonal mean thermal structure predicted by the model.

The effect of such a correction is illustrated in Fig. 4, which shows a set of time series of forecast verifications (rms  $\Delta T$  on the 30 Pa surface, averaged over the globe) for different values of  $\tau$ . The original error growth curve using the uncorrected model is shown as the thick solid line (cf Fig. 3), while empirically

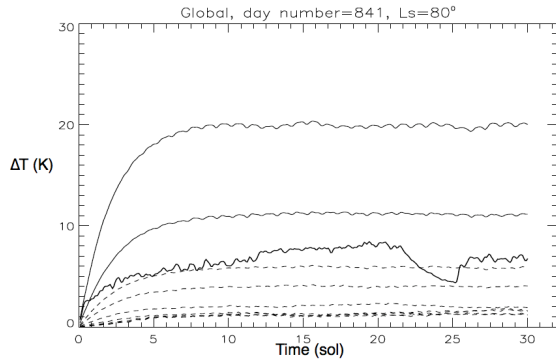


Figure 4: Time series of the growth of model error starting from an initial assimilated state at  $L_S = 80^\circ$  in MY25. The thick solid line represents the rms temperature difference at 30 Pa between uncorrected model forecast and the corresponding assimilated analysis, while other curves represent 'corrected' forecasts with differing values of  $\tau$  ranging from  $< 1$  sol (solid lines) to  $> 1$  sol (dashed lines).

corrected forecasts are shown in thin solid and dashed lines. From this, it is clear that the correction term can have a strong effect on the accuracy of the forecast. In particular, for  $\tau < 1$  sol the correction term is too strong, causing the 'corrected' forecast to drift even further from the assimilated observations than before. For  $\tau > 1$  sol, however, the drift of the model away from the observations is ameliorated and, for  $\tau \sim 30$ –40 sols, the error growth saturates at just a few K. In this case, the error growth and saturation is much closer to that found within the model-only ensemble. This indicates that the divergence of the 'corrected' model is now dominated by internal dynamics, rather than by model systematic errors as in the uncorrected forecast.

The case illustrated here is just one example where a simple zonal mean correction to the heat balance of the model can lead to a significant improvement in the forecast performance. At other times of year, however, the effect of this kind of correction to the zonal mean thermal field was found to be much less effective. Such a result suggests that not all forecast drift may be due to problems with the zonal mean thermal field predicted by the model, but that other features of the model may also exhibit systematic errors that require a different form of correction.

**Conclusions:** In this paper, we have reported on some initial attempts to carry out deterministic numerical weather forecasts for Mars, using a comprehensive Mars GCM initialised from the best available assimilated analyses of observations of the Martian atmosphere. The results indicate that the divergence of ensembles of model forecasts, perturbed about the initial

state, are dominated by internal, chaotic, nonlinear dynamics, leading to a clear sensitivity to initial conditions and a growth rate that depends on season.

Where numerical forecasts are verified against subsequent observations following the initial state, the forecast error is typically found to grow rapidly on timescales comparable with the radiative relaxation timescale. Small errors in the radiative balance of the atmosphere as represented in the model leads to coherent 'climate drift' away from the observations on very short timescales. This starkly demonstrates that Mars poses some very stringent challenges to modellers hoping to produce practical forecasts of sufficient accuracy to be useful. However, some preliminary experiments presented here indicate that, given a more accurate representation of this radiative balance in the model, the scope for improving the performance of the forecasts may be considerable. Future work will need to concentrate on identifying and isolating the main sources of model deficiencies in order to produce forecasting systems of practical utility.

#### References:

- [1] J. R. Barnes. (1980) *J. Atmos. Sci.*, 37:2002–2015.
- [2] J. R. Barnes. (1981) *J. Atmos. Sci.*, 38:225–234.
- [3] C. B. Leovy. (1985) *Adv. Geophys.*, 28a:327–346.
- [4] R. Hide and P. J. Mason. (1975) *Adv. in Phys.*, 24:47–99.
- [5] P. L. Read, M. Collins, W.-G. Fruh, S. R. Lewis & A. F. Lovegrove. (1998) *Chaos, Solitons & Fractals*, 9:231–249.
- [6] M. Collins, S. R. Lewis, P. L. Read, and F. Hourdin. (1996) *Icarus*, 120:344–357
- [7] C. E. Newman, P. L. Read, and S. R. Lewis. (2004) *Quart. J. R. Meteorol. Soc.*, 130:2971–2989.
- [8] Z. Toth and E. Kalnay. (1993) *Bull. Am. Met. Soc.*, 74:2317–2330.
- [9] S. R. Lewis, M. Collins, and P. L. Read. (1996) *Plan. Space Sci.*, 44:1395–1409.
- [10] L. Montabone, S. R. Lewis, P. L. Read, and D. P. Hinson. (2006) *Icarus*, 185:113–132.
- [11] S. R. Lewis, P. L. Read, B. J. Conrath, J. C. Pearl, and M. D. Smith. (2007) *Icarus*, 192:327–347.
- [12] F. Forget, F. Hourdin, R. Fournier, C. Hourdin, O. Talagrand, M. Collins, S. R. Lewis, P. L. Read, and J.-P. Huot. (1999) *J. Geophys. Res.*, 104(E10):24155–24176.
- [13] P. L. Houtekamer and J. Derome. (1994) *Mon. Weather Rev.*, 122:2179–2191.
- [14] R. Goody and M. J. S. Belton (1967) *Plan. Space Sci.*, 15:247–256.
- [15] R. J. Wilson, S. R. Lewis, L. Montabone, M. D. Smith (2008) *Geophys. Res. Lett.*, 35: doi:10.1029/2002GL032405.